International Journal of Environment and Climate Change

Volume 13, Issue 10, Page 1860-1875, 2023; Article no.IJECC.104210
ISSN: 2581-8627
(Past name: British Journal of Environment & Climate Change, Past ISSN: 2231–4784)

Performance of Qualitative and Quantitative Models in Creating Landslide Susceptibility Map of Chaliyar River Basin

L. Aiswarya [a++*], K. P. Rema [a#] and J. Asha [a#]

[a] Department of IDE, KCAET, Tavanur, India.

Authors' contributions

This work was carried out in collaboration among all authors. All authors read and approved the final manuscript.

Article Information

DOI: 10.9734/IJECC/2023/v13i102842

Open Peer Review History:
This journal follows the Advanced Open Peer Review policy. Identity of the Reviewers, Editor(s) and additional Reviewers, peer review comments, different versions of the manuscript, comments of the editors, etc are available here: https://www.sdiarticle5.com/review-history/104210

Original Research Article

Received: 13/06/2023
Accepted: 17/08/2023
Published: 01/09/2023

ABSTRACT

A Landslide Susceptibility Map (LSM) for Kerala's Chaliyar river basin is what this study aims to provide. Several landslides occurred in this basin as a result of the floods in 2018 and 2019. There were 592 identified landslides. Using ArcGIS 10.7 software, the landslide inventory was taken from the inventories created by the National Remote Sensing Center (NRSC) and Kerala State Disaster Management Authority (KSDMA), and the future incidence of landslides was projected by linking the landslide cause variables. Landslide inventories were split into training and validation groups in this study, with the ratios fixed at 70:30. Two models, including a qualitative one called Weighted Linear Combination (WLC) and a quantitative one (a bivariate statistical model) called Weights of Evidence (WOE) model, were used to evaluate landslide susceptibility. The following factors were employed as causative parameters: Slope, Aspect, Curvature, Relative Relief, TWI, Distance to Road, Distance to Streams, Distance to Lineaments, Land Use Land Cover, Drainage Density,

---

[++] *Ph.D Scholar;*
[#] *Professor;*
**Corresponding author: E-mail: aiswaryasona1234@gmail.com, aiswaryasona@gmail.com;*

Road Density, Lineament Density, Geomorphology, Soil Texture, and NDVI. The performance of the models was evaluated using the Receiver Operating Characteristic (ROC)'s Area Under the Curve (AUC). In the study, the WLC model yields an AUC success rate accuracy of 59.9%, while the WOE model yields an accuracy of 70.9%. In terms of ratio of landslide validation accuracy, the WOE model outperforms the WLC model by 11%. The anticipated landslide area is included in the landslide susceptibility map, which can be incorporated to lessen the risk of landslides in this research.

Keywords: Landslide susceptibility; weighted linear combination; weights of evidence; causative parameters; ROC-AUC; Chaliyar river basin.

1. INTRODUCTION

Landslides are devastating natural occurrences that commonly result in substantial issues in hilly areas, resulting in significant harm to natural resources as well as the loss of life and property [1,2] Many portions of India's steep topography, particularly in the Himalayas, Western Ghats, Eastern Ghats, and Vindhyans, are susceptible to landslides (NDMA, 2004). The occurrence of slides and mass wasting in the Himalayan and Western Ghats regions has lately increased due to deforestation and anthropogenic activity, along with unsustainable development projects and damaging practises, necessitating preventative and mitigating measures [3].

Landuse planning includes hazard and risk zoning as well as landslide vulnerability of the study area. Landslide susceptibility mapping is the initial step in reducing the risk of landslides by providing necessary data to support decisions about urban growth, which significantly lowers the risk of landslide damage. In other words, the creation of landslide susceptibility maps serves to aid human recognition and adaptation to landslide hazard mitigation strategies (Pourghasemi et al. 2012). Nevertheless, such a strategy is predicated on the notion that future landslides take place in conditions that are comparable to those seen in the past (Clerici et al. 2006) [4] Up until this point, numerous researchers have worked to improve the precision of landslide susceptibility mapping. Numerous techniques, including both qualitative and quantitative modelling, have been used.

Climate, hydrology, lithology, structure, and geomorphic history are some of the major variables that can affect the likelihood of a slide, although it is not always possible to account for every facet of these variables when determining susceptibility [5].

There are number of methodologies used in the GIS-assisted landslide susceptibility mapping process that may be classified as either qualitative or quantitative. Qualitative methods rely on professional judgement and are frequently helpful for regional assessments (van Westen, et al. 2003). The Weighted Linear Combination (WLC) is one of the qualitative models . This method divides each layer utilised in landslide susceptibility zoning into smaller elements, which are then weighted according to their significance, before the prepared layers are finally merged to create the final map. It is founded on three guiding principles: decomposition, comparative analysis, and priority synthesis. The accuracy of the expert's judgement determines the weight of each layer in this process, and the more accurate the judgement, the more accurate the map that results.

The present approaches employed in the landslide susceptibility evaluation studies was based on quantitative methods that makes relationship between causative factors and landslides [6,7,8]. The investigation also utilised the Weights of Evidence (WoE) modelling method, a bivariate statistical technique that provides a flexible mechanism to examine the significance of input elements for landslide susceptibility.

By identifying and mapping the slide locations and the associated terrain attributes, the current study shows how to apply weighted linear combination (WLC) and weights of evidence (WoE) models to produce a landslide susceptibility zonation map for the Chaliyar river basin at a scale of 1:50,000 for the study area. The objective of this study is to validate the model's applicability and the validity of the resulting landslide susceptibility zonation map.

2. MATERIALS AND METHODS

2.1 Study Area

The Chaliyar River Basin in Kerala, India, which is located between latitudes 11°06' and 11°36'N and 75°48' and 76°33'E, is covered by toposheets 58A and 49M of the Survey of India (SOI). The Chaliyar River, which originates in Tamil Nadu's Nilgiri district at a height of roughly 2560 metres above mean sea level, is the fourth-largest river in Kerala (MSL). The river, known as the Beypore River, flows naturally along the northern border of the Malappuram district through the towns of Nilambur, Mambad, Edavanna,Areakode, and Feroke before joining the Lakshadweep Sea south of Kozhikode, close to Beypore.

2.2 Data Collection

The data collection for landslide susceptibility mapping divided into two groups as:

2.2.1 Landslide inventory

A landslide inventory map is prepared through multiple sources ; (1) National Remote Sensing Center (NRSC), of the Indian Space Research Organization (ISRO), (2) Geological Survey of India (GSI) in collaboration with the Kerala State Disaster Management Authority (KSDMA), (3) BHUVAN (Indian earth observation visualization), a web-based geospatial platform developed by the Indian Space Research Organization (ISRO) (bhukosh.gsi.gov.in). A total of 592 landslides are identified and divided into 70%–30% proportion for training and testing the models [9,10]. In this study field evaluation of the landslide locations were not done.

2.2.2 Causative factors of landslide

In susceptibility mapping, there are no set rules for choosing the variables that affect landslides [11] Based on earlier landslide studies (Martha et al. 2018, [12,13] the scope of the analysis, the availability of data, and fieldwork in the Chaliyar river basin, the causative factors were chosen. Based on literatures and official reports on the mapping of landslide susceptibility in Kerala [14,15,16]. The most significant landslide causative factors namely geomorphology, soil type, Land Use Land Cover (LULC), slope angle, aspect, curvature, relative relief, Topographic Wetness Index (TWI), distance to lineaments, distance to streams, distance to roads, drainage density, lineament density and Normalized Difference Vegetation Index (NDVI) , were selected for this study area. The research area's geomorphology map is obtained from the Kerala State Remote Sensing and Environment Center (scale 1:50,000). Data on land use and land cover are gathered for the research region from the Kerala State Land Use Board (scale 1:50,000). The ASTER GDEM is used to calculate terrain metrics like slope angle, aspect, curvature, relative relief, streams, lineaments, and TWI (30m resolution). Data on the research area's soil texture are gathered from KSDMA, Trivandrum, and the Department of Soil Survey & Soil Conservation. Data on roads were gathered from KSDMA in Trivandrum. The United States Geological Survey's (USGS) Landsat 8 Operational Land Imager (OLI) satellite data was used to create NDVI. The same coordinate system (WGS 1984 UTM zone 43N) and pixel size (30mx30m) were used to create raster maps of all causative factor maps [13]. The fifteen thematic layers of the causal factors applied in this study are depicted in Fig. 2. The spatial analyst tool of ArcGIS was used to extract information from the rasterized training (70%) landslide map and all of the causative component maps in order to determine the ratings or weights of all factor classes for WLC and WoE models. To assess the spatial link between factors and landslide locations in the research area, these ratings or weights of each landslide factor will be added up.

2.3 Landslide Susceptibility Mapping

Landslide susceptibility mapping typically entails the following steps: (1) gathering data and building a spatial database of the landslide causative factors; (2) developing a landslide inventory; and (3) using a model or approach to evaluate the landslide susceptibility according to the relationship between landslides and its causative factors; and (4) validating the resulting landslide susceptibility map [17]. Weighted Linear Combination (WLC) and Weights of Evidence (WOE) models were the two models used in the study. Fig. 3 depicts the research process flowchart.

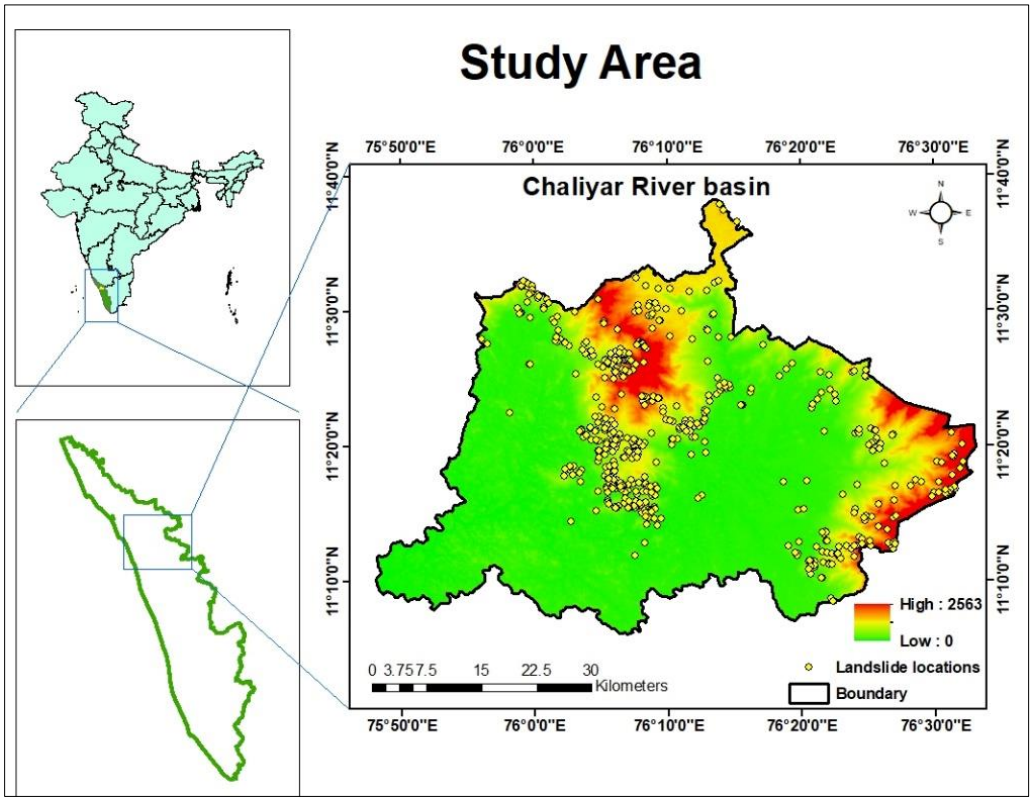

Fig.1 Location map of the study area showing the elevation and landslide inventory

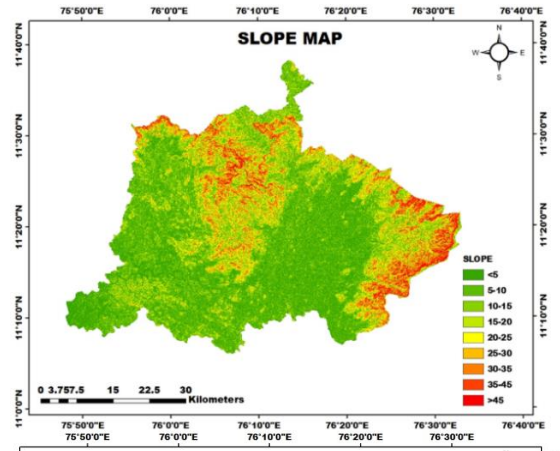

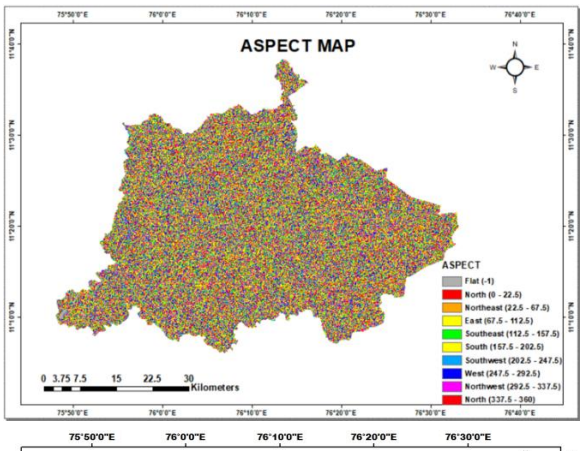

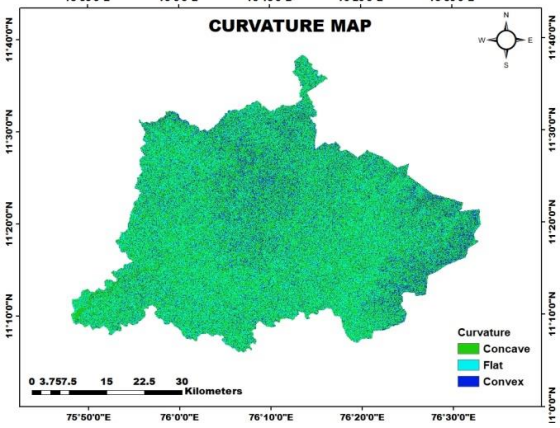

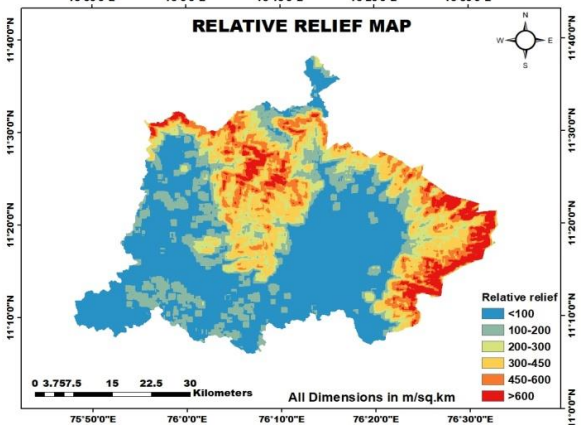

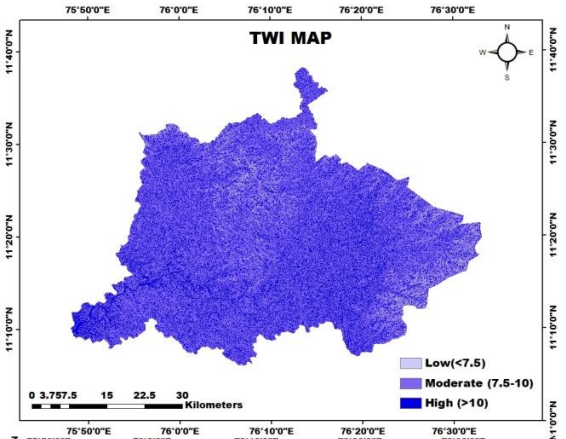
TWI MAP
Low(<7.5)
Moderate (7.5-10)
High (>10)
0 3.757.5 15 22.5 30
Kilometers

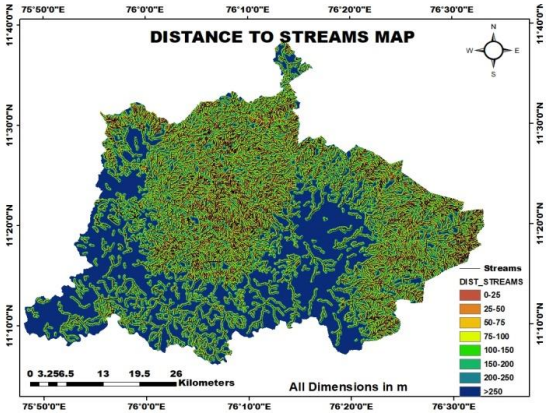
DISTANCE TO STREAMS MAP
Streams
DIST_STREAMS
0-25
25-50
50-75
75-100
100-150
150-200
200-250
>250
0 3.256.5 13 19.5 26
Kilometers
All Dimensions in m

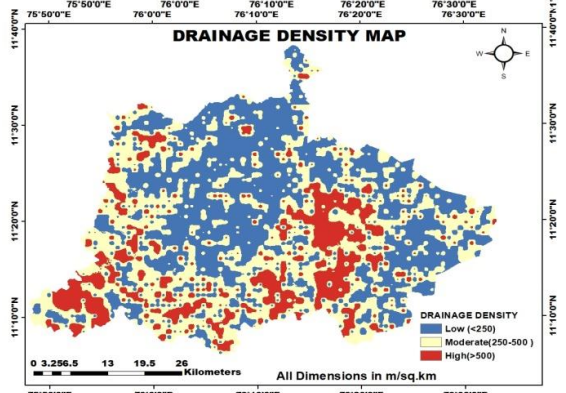
DRAINAGE DENSITY MAP
DRAINAGE DENSITY
Low (<250)
Moderate(250-500)
High(>500)
0 3.256.5 13 19.5 26
Kilometers
All Dimensions in m/sq.km

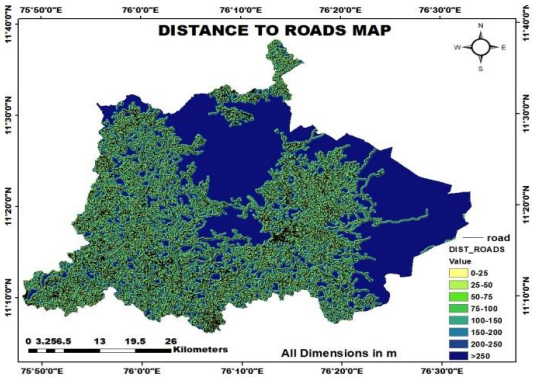
DISTANCE TO ROADS MAP
road
DIST_ROADS
Value
0-25
25-50
50-75
75-100
100-150
150-200
200-250
>250
0 3.256.5 13 19.5 26
Kilometers
All Dimensions in m

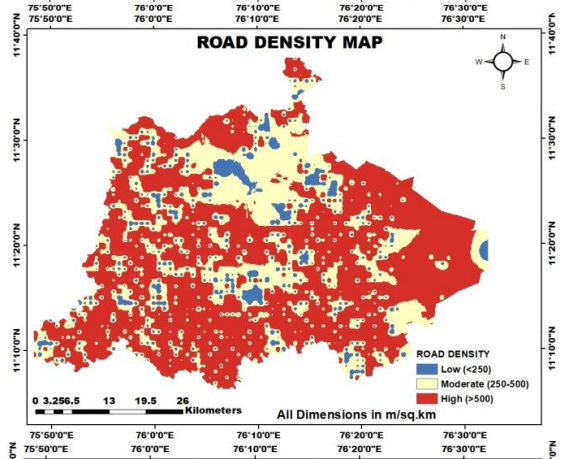
ROAD DENSITY MAP
ROAD DENSITY
Low (<250)
Moderate (250-500)
High (>500)
0 3.256.5 13 19.5 26
Kilometers
All Dimensions in m/sq.km

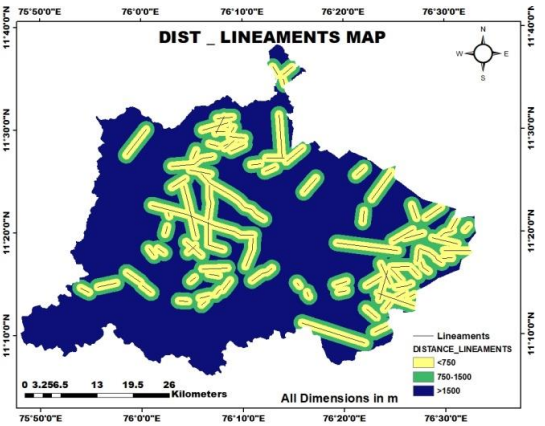
DIST _ LINEAMENTS MAP
Lineaments
DISTANCE_LINEAMENTS
<750
750-1500
>1500
0 3.256.5 13 19.5 26
Kilometers
All Dimensions in m

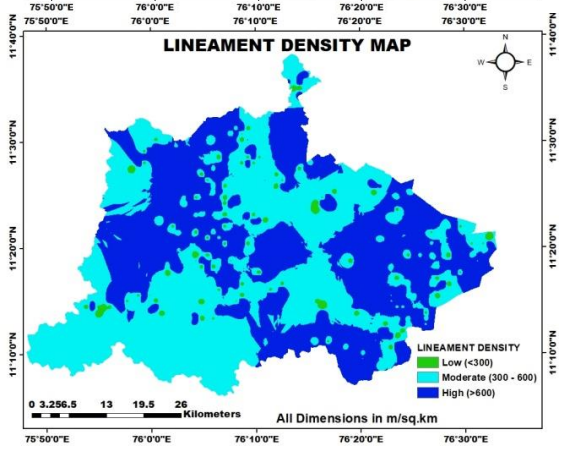
LINEAMENT DENSITY MAP
LINEAMENT DENSITY
Low (<300)
Moderate (300 - 600)
High (>600)
0 3.256.5 13 19.5 26
Kilometers
All Dimensions in m/sq.km

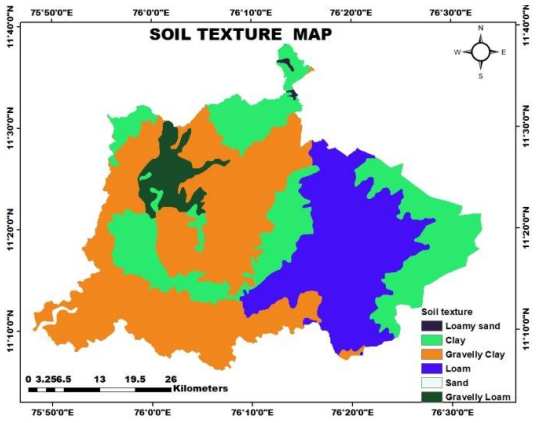
SOIL TEXTURE MAP
Soil texture
Loamy sand
Clay
Gravelly Clay
Loam
Sand
Gravelly Loam
0 3.256.5 13 19.5 26
Kilometers

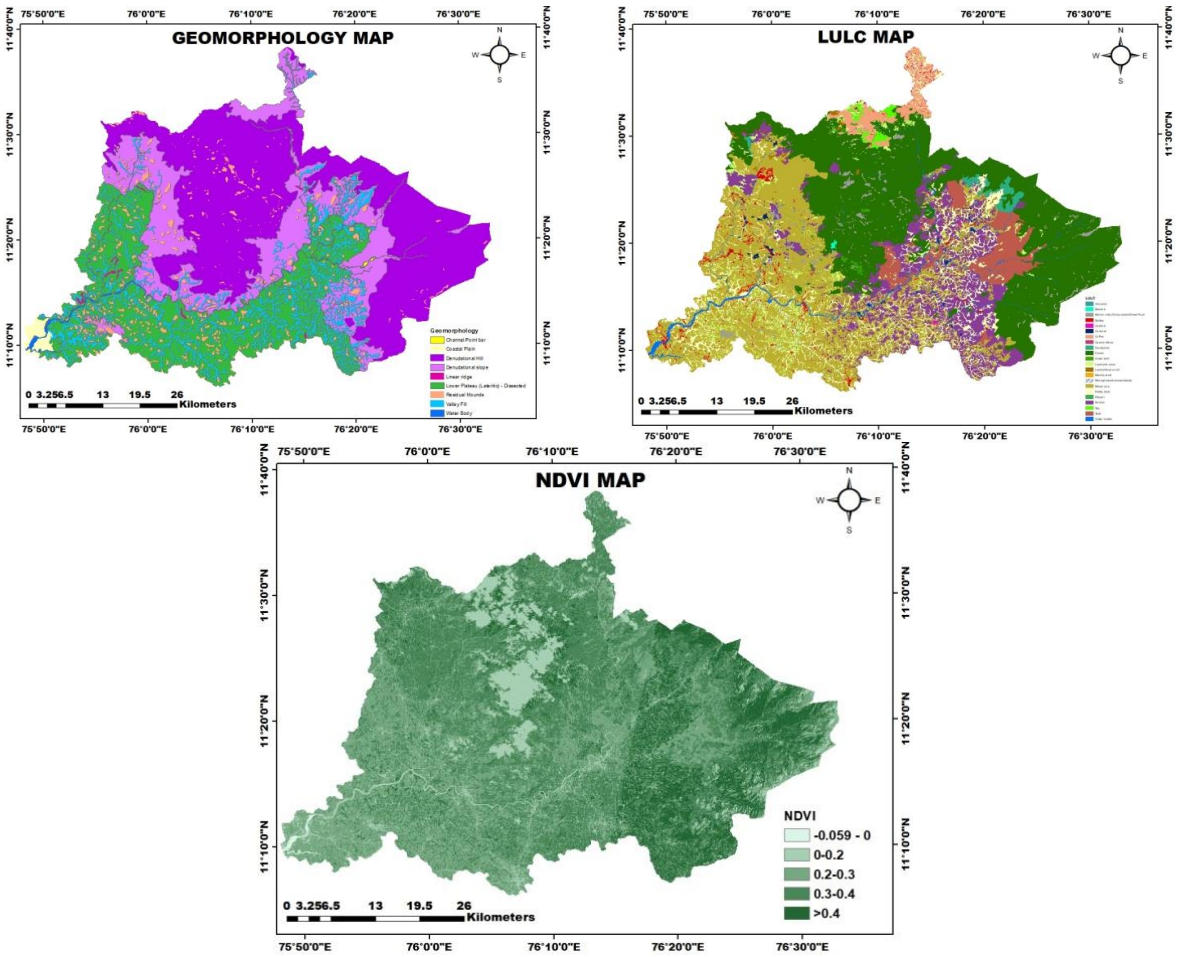

Fig 2. Fifteen landslide causative factors used in this study

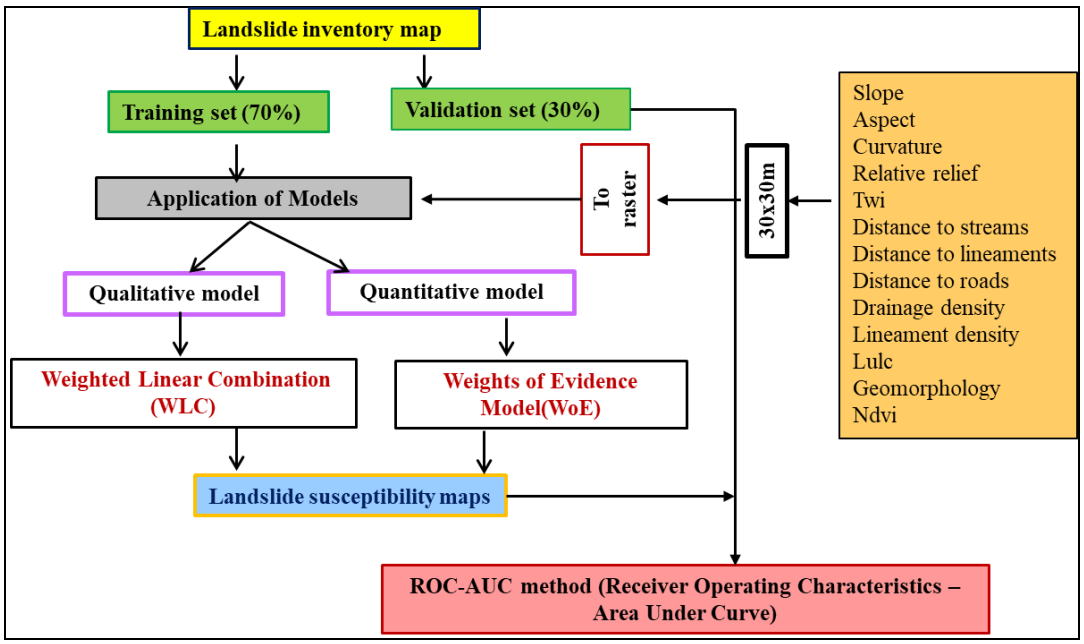

Fig. 3. Flowchart of the research work

2.3.1 Weighted Linear Combination (WLC) model

WLC model is a data-driven analytical method involving several parameters were used in order to determine the relative importance and level of influence of the chosen parameters to permit a landslide event in a GIS environment. There are no predetermined standards; only professional knowledge is used for assigning weights to the factors. In a GIS overlay environment, each parameter is classified, multiplied by its assigned weight, and the weighted averages are added to produce the final output map. In WLC, the weight of each parameter taken into account is added using overlay as follows:

$$S = \sum_{i=1}^{n} W_i X_i$$

Where, W_i is the weight of factors and X_i is the criterian score of the factor.

The final output is typically a map that shows the spatial distribution of landslide susceptibility in the study area. The map can be useful for land use planning and natural resource management. However, it is important to note that the accuracy of the WLC method depends on the quality and quantity of data used, as well as the expertise of the analyst in selecting the appropriate factors and assigning the appropriate weights.

2.3.2 Weights of Evidence (WOE) model

The weight of evidence (WoE) method was a data-driven approach to identifying the causative factors that does not depend on the expert opinion for assigning weight. The premise behind this approach is that "the past is the key to the future." Hence, it is anticipated that comparable factors that contributed to earlier landslides will be present in future landslides. It is assumed that the combination of causative factors of landslides is conditionally independent of one another (Sifa et al. 2019). Also, it is assumed that the confluence of causative elements may have caused earlier landslides in the current research area. As a result, the elements that mostly contribute to or cause landslides were weighted using data from previous landslides. Based on the presence (W+) or absence (W-) of landslides in the area, the WoE technique provides a weight to each class of a landslide's causative component [18]. This approach uses a correlation between positive weights (W+) when the event happens and negative weights (W-) when it doesn't, where W+ and W- are defined as:

$$W^{+} = \log_e \frac{P\left\{\frac{B}{D}\right\}}{P\left\{\frac{B}{\overline{D}}\right\}}$$

$$W^{-} = \log_e \frac{P\left\{\frac{\overline{B}}{D}\right\}}{P\left\{\frac{\overline{B}}{\overline{D}}\right\}}$$

where P is the probability, B is the presence of a desired class of landslide causative factor, $\overline{B}$ is the absence of a desired class of landslide causative factor, D is the presence of landslides, and $\overline{D}$ is the absence of a landslides. Since the results are in log form. As a result, the weight contrast, abbreviated C, is the difference between the two weights (C = W+ - W-). The size of the contract shows how far dispersed the causal variables and the landslides are in space. The standardised value of C is determined by dividing it by the standard deviation, or S(C) [19,20]. The significance of the spatial link between elements influencing the incidence of a landslide is determined by the value of Wstd. It also displays the posterior probability's relative certainty [21]. The following formula is used to calculate the S(C) (standard deviation) of positive and negative weights:

$$S(C) = \sqrt{S^2\, W^{+} + S^2 W^{-}}$$

The factor is favourable for landslides if the weight contrast is positive, and it is unfavourable for landslides if it is negative. The factor has little bearing on the landslides if the weight contrast is close to zero. The landslide susceptibility index (LSI) map was developed by averaging the standardised (W_{std}) weight contrasts of each causative element as follows: LSI = SW_{std} (where W_{std} = standardised weight contrast of each factor). A landslide's susceptibility is high when the LSI value is high or positive, and a landslide's susceptibility is low when the LSI value is low or negative.

2.4 Validation of Landslide Susceptibility Map

The validation is required to create an accurate map of landslide susceptibility and identify the best suitable model. The relative operative characteristic (ROC) approach and the proportion of observed landslides in various susceptibility categories were used to assess the validity of the landslide susceptibility map. The area under the curve (AUC) of the ROC shows the quality of the probabilistic model (its ability to forecast the occurrence or non-occurrence of an event [22]. AUC values near 1 imply great

accuracy, whereas values near 0.5 denote inaccuracy [23-25].

3. RESULTS AND DISCUSSION

3.1 Relationship between Landslide and Causative Factors

In this study, the correlation between fifteen potential causative factors of landslides and their occurrence was examined. For both the WLC and WoE models, the causative factors were divided into various classes and given weights, as shown in Tables 1 and 2, respectively.

3.2. Landslide Susceptibility Map

The landslide susceptibility maps were obtained using the WLC and WoE method. Each parameter identified as influencing landslide occurrence in the Chaliyar river basin was evaluated, classified, and ranked independently using the WLC approach. Weights were assigned to each parameter based on how much influence they had on landslides in comparison to other parameters (Table 1), and utilising GIS overlay functionality, a weighted sum was calculated to integrate all the parameters. In the ArcGIS weighted sum environment, Fig. 4a displays the results (LSI map) of combining several weighted parameters using the WLC approach. This approach produces an LSI map with a value range of 0.087 to 0.311. The map is then categorised as a Landslide Susceptibility Zonation (LSZ) map, with five classes (Very low, low, moderate, high, and very high) based on literatures. The classes that result are very low (39.58%), low (18.14%), moderate (23.02%), high (13.60%), and very high (5.66%) according to the degree of susceptibility [26-28].

Table 1. Data analyses and results obtained from WLC model

Sl No.	Factors	Class	Weights
1	Slope	0-5	0.010
		5-10	0.020
		10-15	0.060
		15-20	0.090
		20-25	0.130
		25-30	0.140
		30-35	0.170
		35-45	0.180
		>45	0.200
2	Aspect	Flat(-1)	0.003
		North(0-22.5)	0.099
		Northeast(22.5-67.5)	0.131
		East(67.5-112.5)	0.156
		Southeast(112.5-157.5)	0.115
		South(157.5-202.5)	0.140
		Southwest(202.5-247.5)	0.082
		West(247.5-292.5)	0.090
		Northwest(292.5-337.5)	0.085
3	Curvature	Concave	0.476
		Flat	0.095
		Convex	0.429
4	Relative relief	<100 m/km^2	0.015
		100-200 m/km^2	0.060
		200-300 m/km^2	0.149
		300-450 m/km^2	0.299
		450-600 m/km^2	0.269
		>600 m/km^2	0.209
5	TWI	Low (5.6 - 7.5)	0.129
		Moderate (7.5-10)	0.516
		High (10-23)	0.355
6	Distance to drainage	0-25 m	0.220
		25-50 m	0.209
		50-75 m	0.176

Sl No.	Factors	Class	Weights
		75-100 m	0.165
		100-150 m	0.110
		150-200 m	0.066
		200-250 m	0.044
		>250 m	0.011
7	Drainage Density	Low (<250 m/km2)	0.516
		Moderate (250-500 m/km2)	0.387
		High (>500 m/km2)	0.097
8	Distance to road	0-25 m	0.220
		25-50 m	0.198
		50-75 m	0.187
		75-100 m	0.154
		100-150 m	0.121
		150-200 m	0.066
		200-250 m	0.044
		>250 m	0.011
9	Road density	Low (<250 m/km^2)	0.235
		Moderate (250-500 m/km^2)	0.353
		High (>500 m/km^2)	0.412
10	Dist.Lineaments	500 - 750 m	0.516
		750- 1500 m	0.355
		>1500 m	0.129
11	Lineament density	Low (<300 m/km2)	0.103
		Moderate (300-600 m/km2)	0.310
		High (>600 m/km2)	0.586
12	Geomorphology	Channel/Point bar	0.000
		Coastal Plain	0.000
		Denuational Hill	0.429
		Denudational slope	0.310
		Linear ridge	0.000
		Lower Plateau(Lateritic)- Dissected	0.238
		Residual mounds	0.024
		Valley Fill	0.000
		Water body	0.000
13	Land use Land cover	Arecanut	0.000
		Banana	0.000
		Barren rocky/stonywaste/sheetrock	0.000
		cashew	0.021
		coconut	0.000
		coffee	0.053
		current fallow	0.011
		Eucalyptus	0.011
		Forest	0.181
		Grassland	0.064
		Land with scrub	0.128
		Land without scrub	0.138
		Marshy land	0.000
		Mining/Industrial wasteland	0.000
		Builtup	0.000
		Mixed crop	0.160
		Paddy land	0.000
		Pepper	0.011
		Rubber	0.096
		Tea	0.074
		Teak	0.053
		Waterbodies	0.000

Sl No.	Factors	Class	Weights
14	Soil texture	Clay	0.286
		Gravelly clay	0.257
		Gravelly loam	0.214
		Loam	0.157
		Loamy sand	0.071
		Sand	0.014
15	NDVI	-0.059-0	0.000
		0-0.2	0.045
		0.2-0.3	0.227
		0.3-0.4	0.318
		>0.4	0.409

Table 2. Data analyses and results obtained from WoE model

Factor	CLASS	W+	S_W+	W-	S_W-	C	S(C)	WEIGHT	W_{Std}
Slope	0-5°	-1.941	0.289	0.196	0.050	-2.137	0.293	-1.941	0.289
	5-10°	-1.587	0.209	0.260	0.051	-1.846	0.215	-1.587	0.209
	10-15°	-0.370	0.141	0.064	0.052	-0.434	0.151	-0.370	0.141
	15-20°	0.431	0.117	-0.072	0.054	0.503	0.129	0.431	0.117
	20-25°	0.743	0.119	-0.103	0.054	0.846	0.130	0.743	0.119
	25-30°	0.985	0.124	-0.110	0.054	1.095	0.135	0.985	0.124
	30-35°	1.057	0.143	-0.084	0.052	1.141	0.152	1.057	0.143
	35-45°	1.027	0.143	-0.083	0.052	1.109	0.152	1.027	0.143
	>45°	1.385	0.213	-0.041	0.051	1.426	0.219	1.385	0.213
Aspect	Flat	0.000	0.000	0.000	0.000	0.000	0.000	-0.348	0.167
	North	0.079	0.183	-0.006	0.051	0.085	0.190	-0.348	0.167
	Northeast	0.102	0.134	-0.015	0.053	0.118	0.144	-0.348	0.167
	East	0.220	0.128	-0.034	0.053	0.253	0.139	-0.348	0.167
	Southeast	-0.170	0.153	0.022	0.052	-0.192	0.161	-0.348	0.167
	South	0.156	0.123	-0.027	0.054	0.183	0.134	-0.348	0.167
	Southwest	-0.348	0.167	0.040	0.051	-0.388	0.174	-0.348	0.167
	West	-0.023	0.144	0.003	0.052	-0.026	0.154	-0.348	0.167
	Northwest	0.010	0.140	-0.001	0.053	0.011	0.150	-0.348	0.167
Curvature	Concave	0.000	0.067	0.000	0.072	0.000	0.099	0.000	0.072
	Flat	-0.247	0.099	0.097	0.057	-0.345	0.114	-0.247	0.099
	Convex	0.386	0.105	-0.085	0.056	0.472	0.119	0.386	0.105
Relative relief	<100 m/km^2	-2.664	0.277	0.568	0.050	-3.232	0.282	-2.664	0.277
	100-200 m/km^2	-1.049	0.204	0.121	0.051	-1.170	0.210	-1.049	0.204
	200-300 m/km^2	1.012	0.095	-0.210	0.058	1.222	0.111	1.012	0.095
	300-450 m/km^2	0.832	0.086	-0.246	0.060	1.079	0.105	0.832	0.086
	450-600 m/km^2	0.531	0.127	-0.070	0.053	0.601	0.138	0.531	0.127
	>600 m/km^2	1.094	0.122	-0.121	0.054	1.215	0.134	1.094	0.122
TWI	Low (5.6 - 7.5)	1.193	0.156	-0.074	0.052	1.266	0.165	1.193	0.156
	Moderate (7.5-10)	0.030	0.060	-0.062	0.087	0.092	0.106	-0.061	0.087
	High (10-23)	-0.341	0.105	0.121	0.056	-0.462	0.119	-0.341	0.105
Distance to streams	0-25 m	0.345	0.143	-0.038	0.052	0.383	0.152	0.345	0.143
	25-50 m	0.172	0.113	-0.037	0.055	0.209	0.125	-0.086	0.066
	50-75 m	0.457	0.120	-0.071	0.054	0.528	0.132	0.457	0.120
	75-100 m	0.130	0.153	-0.014	0.052	0.144	0.161	-0.086	0.066
	100-150 m	0.315	0.112	-0.063	0.055	0.378	0.125	0.315	0.112
	150-200 m	0.126	0.169	-0.011	0.051	0.137	0.177	-0.086	0.066
	200-250 m	-0.046	0.196	0.003	0.051	-0.049	0.203	-0.086	0.066
	>250 m	-1.247	0.174	0.242	0.051	-1.489	0.182	-1.247	0.174

Factor	CLASS	W+	S_W+	W-	S_W-	C	S(C)	WEIGHT	W_{Std}
Distance to lineaments	>250 m	0.605	0.079	-0.249	0.063	0.855	0.101	0.605	0.079
	500 - 750 m	0.351	0.156	-0.032	0.052	0.383	0.165	0.351	0.156
	750- 1500 m	-0.332	0.068	0.548	0.071	-0.880	0.098	-0.332	0.068
Distance to Roads	0-25 m	0.474	0.123	-0.069	0.054	0.543	0.134	0.474	0.123
	25-50 m	-0.632	0.167	0.088	0.051	-0.720	0.174	-0.632	0.167
	50-75 m	-1.041	0.267	0.066	0.050	-1.107	0.272	-1.041	0.267
	75-100 m	-0.731	0.258	0.041	0.050	-0.772	0.263	-0.731	0.258
	100-150 m	-0.050	0.154	0.006	0.052	-0.056	0.163	0.042	0.054
	150-200 m	-0.350	0.250	0.017	0.050	-0.367	0.255	0.042	0.054
	200-250 m	-0.310	0.267	0.013	0.050	-0.323	0.272	0.042	0.054
	>250 m	0.352	0.069	-0.269	0.070	0.620	0.098	0.352	0.069
Road Density	Low (<250m/km^2)	0.569	0.144	-0.055	0.052	0.624	0.154	0.5688	0.1444
	Moderate (250-500 m/km^2)	0.150	0.082	-0.075	0.061	0.225	0.103	0.1501	0.0822
	High (>500 m/km^2)	-0.174	0.068	0.238	0.071	-0.412	0.098	-0.1741	0.0677
Drainage density	Low (<250m/km^2)	0.397	0.062	-0.451	0.081	0.848	0.102	0.397	0.062
	Moderate (250-500 m/km^2)	-0.270	0.089	0.147	0.059	-0.417	0.107	-0.270	0.089
	High (>500 m/km^2)	-1.082	0.204	0.128	0.051	-1.210	0.210	-1.082	0.204
Lineament Density	Low (<300 m/km^2)	-0.805	0.577	0.009	0.049	-0.814	0.580	0.009	0.049
	Moderate (300-600 m/km^2)	-0.232	0.078	0.190	0.063	-0.423	0.100	-0.232	0.078
	High (>600m/km^2)	0.211	0.064	-0.246	0.077	0.458	0.100	0.211	0.064
Geomorphology	Channel/Point bar	0.767	0.052	-1.589	0.141	2.355	0.151	0.767	0.052
	Coastal Plain	-2.128	0.500	0.075	0.049	-2.203	0.502	-2.128	0.500
	Denuational Hill	0.282	0.229	-0.012	0.050	0.294	0.235	0.011	0.050
	Denudational slope	-1.332	0.209	0.179	0.051	-1.511	0.215	-1.332	0.209
	Linear ridge	0.000	0.000	0.000	0.000	0.000	0.000	0.011	0.050
	Lower Plateau(Lateritic)-Dissected	0.000	0.000	0.000	0.000	0.000	0.000	0.011	0.050
	Residual mounds	-3.226	0.500	0.269	0.049	-3.495	0.502	-3.226	0.500
	Valley Fill	0.000	0.000	0.000	0.000	0.000	0.000	0.011	0.050
	Water body	0.000	0.000	0.000	0.000	0.000	0.000	0.011	0.050
LULC	Arecanut	0.000	0.000	0.000	0.000	0.000	0.000	0.014	0.056
	Banana	0.538	0.065	-0.446	0.075	0.984	0.099	0.538	0.065
	Barren rocky/stonywaste/sheetrock	0.952	0.707	-0.003	0.049	0.955	0.709	0.014	0.056
	cashew	-0.826	0.135	0.219	0.053	-1.045	0.145	-0.826	0.135
	coconut	-0.128	0.148	0.017	0.052	-0.145	0.156	0.014	0.056
	coffee	-0.082	1.000	0.000	0.049	-0.082	1.001	0.014	0.056
	current fallow	-0.558	0.577	0.006	0.049	-0.563	0.580	0.014	0.056
	Eucalyptus	1.597	1.000	-0.002	0.049	1.599	1.002	0.014	0.056
	Forest	0.000	0.000	0.000	0.000	0.000	0.000	0.014	0.056
	Grassland	1.271	0.218	-0.038	0.050	1.309	0.224	1.271	0.218
	Land with scrub	0.715	0.378	-0.009	0.050	0.724	0.381	0.014	0.056

Factor	CLASS	W+	S_W+	W-	S_W-	C	S(C)	WEIGHT	W_{Std}
	Land without scrub	0.267	0.250	-0.009	0.050	0.276	0.255	0.014	0.056
	Marshy land	0.384	0.707	-0.002	0.049	0.386	0.709	0.014	0.056
	Mining/Industrial wasteland	-2.663	0.707	0.067	0.049	-2.730	0.709	-2.663	0.707
	Builtup	0.000	0.000	0.000	0.000	0.000	0.000	0.014	0.056
	Mixed crop	3.151	0.501	-0.009	0.049	3.160	0.503	3.151	0.501
	Paddy land	0.000	0.000	0.000	0.000	0.000	0.000	0.014	0.056
	Pepper	0.000	0.000	0.000	0.000	0.000	0.000	0.014	0.056
	Rubber	0.000	0.000	0.000	0.000	0.000	0.000	0.014	0.056
	Tea	-1.847	0.577	0.040	0.049	-1.887	0.580	-1.847	0.577
	Teak	0.169	0.289	-0.005	0.050	0.174	0.293	0.014	0.056
	Waterbodies	-0.762	1.000	0.003	0.049	-0.765	1.001	0.014	0.056
NDVI	-0.059	0.000	0.000	0.000	0.000	0.000	0.000	0.424	0.135
	0-0.2	0.424	0.135	-0.052	0.053	0.476	0.145	0.424	0.135
	0.2-0.3	0.017	0.081	-0.010	0.062	0.027	0.102	0.424	0.135
	0.3-0.4	-0.069	0.077	0.049	0.064	-0.118	0.100	0.424	0.135
	>0.4	-0.203	0.158	0.024	0.052	-0.228	0.166	0.424	0.135
Soil texture	Clay	0.000	0.000	0.000	0.000	0.000	0.000	-0.066	0.062
	Gravelly clay	0.091	0.088	-0.038	0.059	0.129	0.106	-0.066	0.062
	Gravelly loam	0.118	0.070	-0.101	0.069	0.220	0.098	0.118	0.070
	Loam	-0.526	0.131	0.120	0.053	-0.646	0.142	-0.526	0.131
	Loamy sand	0.000	0.000	0.000	0.000	0.000	0.000	-0.066	0.062

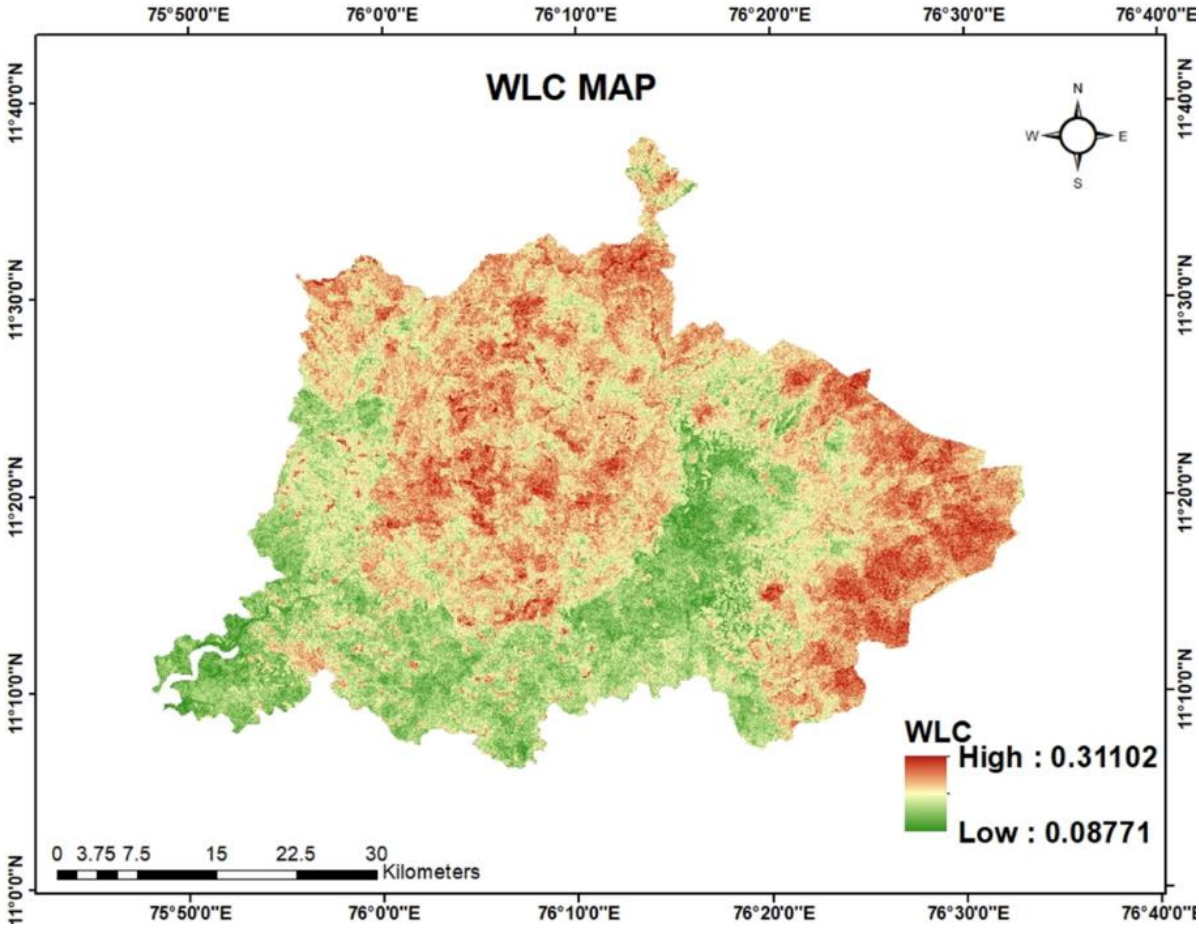

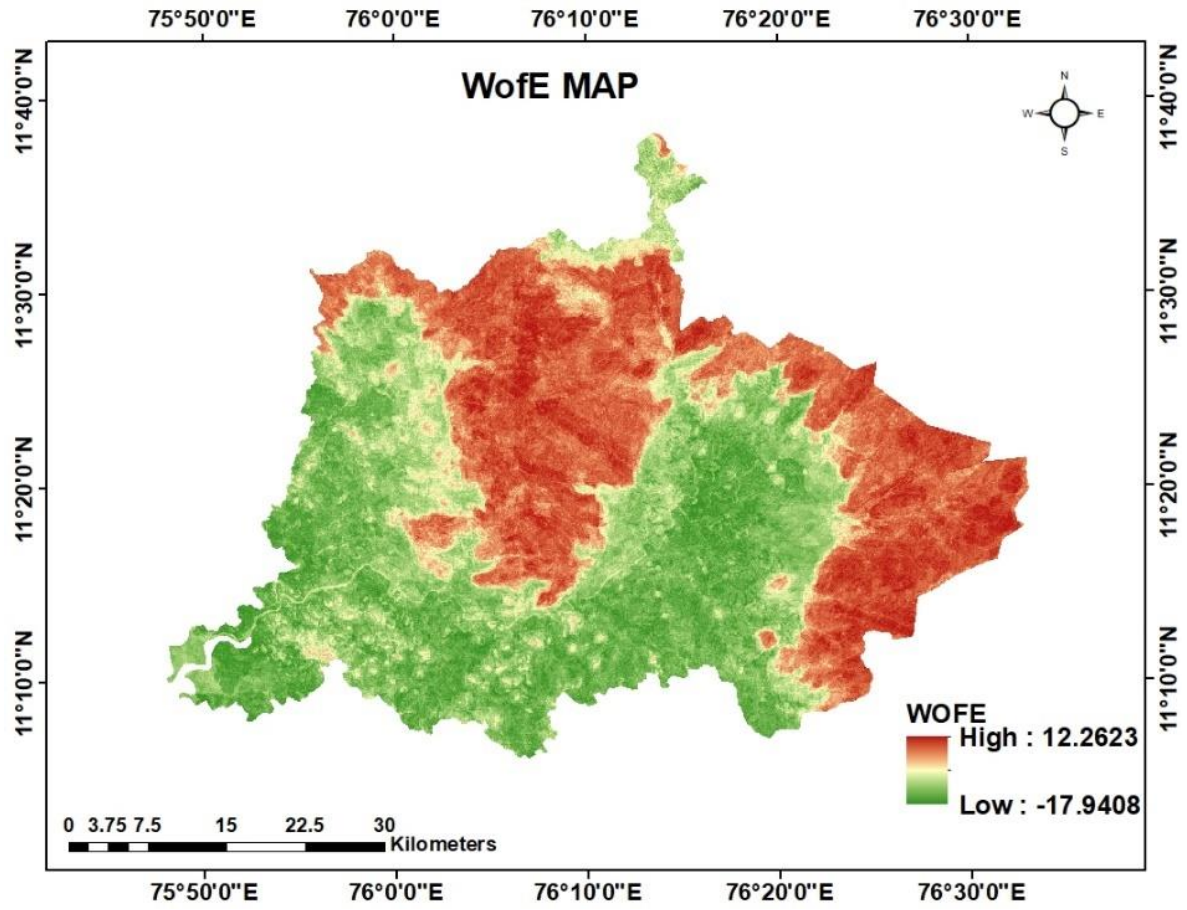

Fig. 4. Landslide susceptibility index (a) WLC model; (b) WOE model

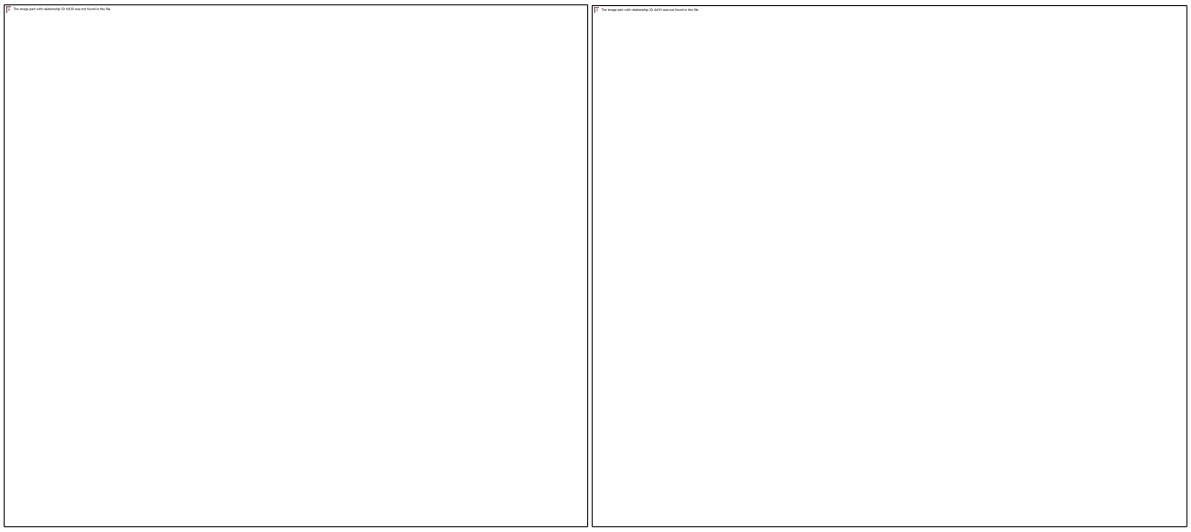

Fig. 5. ROC-AUC performance of models

With regard to the bivariate statistical model, the contrast value that is associated with the landslide probability was set to the weights for each class of evidentiary themes in the created WoE table (Table 2). The classes of each theme are given these weights in order to create weighted thematic maps, which are then layered and numerically added using the equation given below to create a map that shows the landslide susceptibility index (LSI) (Fig. 4b) [29,30].

$LSI_c = \sum F_C$, where, Fc, is the contrast of each factor's range or type.

The study produced an area-specific LSI map by combining each parameter with the raster calculator and adding the themes one at a time to evaluate the impact of each causative factors on the final LSI map, which had values ranging from -17.940 to 12.262. According to Vijith et al. (2014),[2] a high LSI value indicates a higher sensitivity to landslides, whereas a lower number indicates a reduced susceptibility. Using professional judgement, this final LSZ map is once more divided into five classes, producing five susceptibility levels. The area designated as stable, low, moderate, high, and extremely high was then combined with the reclassified susceptibility zone map. The resulting classes are named with the associated degree of susceptibility namely very low (45.59%), low (11.25%), moderate (17.44%), high (17.92%) and very high (7.80%).

3.3 Validation of Landslide Susceptibility Map

A random sample of 30% of landslides were used to test the validity of the landslide susceptibility map. Fig. 5 displays the ROC (AUC) curve for model performance. In comparison to WLC (AUC=0.599), the WoE approach has a high success rate (AUC = 0.709), according to the AUC value.

4. CONCLUSION

The interaction of numerous components leads to the spatial distribution of landslides. The inclusion and appropriate assessment of these criteria' roles are essential to producing a trustworthy and accurate susceptibility map. In this study, fifteen landslide-causative factors were taken into account, including soil texture, geomorphology, LULC, and NDVI, as well as slope, aspect, curvature, relative relief, TWI, relative relief, distance to streams, roads, and lineaments, drainage density, road density, and lineament density. In order to create a landslide susceptibility map using weighted average values, a technique known as weighted linear combination (WLC) was utilised, in which specific classes of each parameter were assessed and factor weights were assigned. The map is then divided into five classes—Very low, low, moderate, high, and very high—under the Landslide Susceptibility Zonation (LSZ) classification system. According to the level of susceptibility they represent, the classifications that emerge are very low (39.58%), low (18.14%), moderate (23.02%), high (13.60%), and very high (5.66%). The analysis also used a statistical model called the Weights of Evidence Model, where the training set served as the predictor layer and thematic layers served as input layers. The resulting classes are named with the associated degree of susceptibility namely very low (45.59%), low (11.25%), moderate (17.44%), high (17.92%) and very high (7.80%) was made possible by the findings of all investigations and evaluations. The landslide susceptibility map is thought to be helpful for locating slope portions that are relative landslide susceptible.

ACKNOWLEDGEMENT

Am thankful to my Chairman, Dr Rema K.P for her guidance and thanks to Kerala State Disaster Management Authority for the training given to me during my research work.

DISCLAIMER

This paper is an extended version of a preprint document of the same author.

The preprint document is available in this link: https://assets.researchsquare.com/files/rs-3193541/v1/6a89b2a9-af63-4ec0-9881 5317adac12dd.pdf?c=1690829521

[As per journal policy, preprint article can be published as a journal article, provided it is not published in any other journal]

COMPETING INTERESTS

Authors have declared that no competing interests exist.

REFERENCES

1. Shavan K, Arunkumar KS, Krishnan MN, Assessment and prediction of shallow landslide susceptibility of Thodupuzha and Peermed Taluks in Idukki district. Kerala;2014.
2. Vijith H, Krishnakumar KN, Pradeep GS, Ninu Krishnan MV, Madhu G. Shallow LANDSLIDE initiation susceptibility mapping by GIS-based weights-of-evidence analysis of multi-class spatial data-sets: A case study from the natural sloping terrain of Western Ghats, India. Georisk: Assessment and Management of

Risk for Engineered Systems and Geohazards. 2014;8(1):48-62.
3. Kuriakose SL, Van Beek LPH, Van Westen, CJ Parameterizing a physically based shallow landslide model in a data poor region. Earth surface processes and landforms. 2009;34(6):867-881.
4. Pandey A, Dabral PP, Chowdary VM, Yadav NK. Landslide hazard zonation using remote sensing and GIS: a case study of Dikrong river basin, Arunachal Pradesh, India. Environmental Geology. 2008;54:1517-1529.
5. Zakharovskyi V, Németh K. Quantitative-qualitative method for quick assessment of geodiversity. Land. 2021;10(9):946.
6. Khan H, Shafique M, Khan MA, Bacha MA, Shah SU, Calligaris C. Landslide susceptibility assessment using Frequency Ratio, a case study of northern Pakistan. The Egyptian J. Remote Sensing and Space Sci. 2019;22(1):11-24.
7. Achu AL, Aju CD, Reghunath R. Spatial modelling of shallow landslide susceptibility: A study from the southern Western Ghats region of Kerala, India. Annals of GIS. 2020;26(2):113-131.
8. Jacinth JJ, Saravanan S. Artificial neural network and sensitivity analysis in the landslide susceptibility mapping of Idukki district, India. Geocarto Int. 2022;37(19):5693-5715
9. Vineetha P, Sarun S. Sheela AM. Landslide susceptibility analysis using frequency ratio model in a tropical region, South East Asia. Journal of Geography, Environment and Earth Science International. 2019;22(2):1-13.
10. Yuvaraj RM, Dolui B. Statistical and machine intelligence based model for landslide susceptibility mapping of Nilgiri district in India. Environmental Challenges. 2021;5:100211.
11. Sato HP, Harp EL. Interpretation of earthquake-induced landslides triggered by the, M7. 9 Wenchuan earthquake in the Beichuan area, Sichuan Province, China using satellite imagery and Google Earth. Landslides. 2008;6:153-159.
12. Banerjee P, Ghose MK, Pradhan R. Analytic hierarchy process and information value method-based landslide susceptibility mapping and vehicle vulnerability assessment along a highway in Sikkim Himalaya. Arabian Journal of Geosciences. 2018;11:1-18.
13. Maheshwari BK.Earthquake-induced landslide hazard assessment of chamoli district, uttarakhand using relative frequency ratio method. Indian Geotechnical Journal. 2019;49108-123.
14. Wadhawan SK, Singh B, Ramesh MV. Causative factors of landslides 2019: case study in Malappuram and Wayanad districts of Kerala, India. Landslides. 2020;17:2689-2697.
15. Gururajan B, nehru Jawaharlal A. Landslide vulnerability assessment in Devikulam Taluk, Idukki District, Kerala Using Gis and Machine Learning Algorithms; 2021.
16. Vishnu CL, Oommen T, Chatterjee S, Sajinkumar KS. Challenges of modeling rainfall triggered landslides in a data-sparse region: A case study from the Western Ghats, India. Geosystems and Geoenvironment. 2022;1(3):100060.
17. Martha TR, Roy P, Govindharaj KB, Kumar KV, Diwakar PG, Dadhwal VK.. Landslides triggered by the June 2013 extreme rainfall event in parts of Uttarakhand state, India. Landslides. 2015;12:135-146.
18. Samia J, Temme A, Bregt AK, Wallinga J, Stuiver J, Guzzetti F, Ardizzone F, Rossi M.. Implementing landslide path dependency in landslide susceptibility modelling. Landslides. 2018;15:2129-2144.
19. Kumar R, Anbalagan R. Landslide susceptibility mapping of the Tehri reservoir rim area using the weights of evidence method. Journal of Earth System Science, 2019;128:1-18.
20. Goetz J, Brenning A, Petschko H, Leopold P. Evaluating machine learning and statistical prediction techniques for landslide susceptibility modeling. Comput. Geosci. 2015;81:1–11.
21. Ding Q, Chen W, Hong H. Application of frequency ratio, weights of evidence and evidential belief function models in landslide susceptibility mapping. Geocarto International. 2017;32(6):619-639.
22. Polykretis C, Ferentinou M, Chalkias C. A comparative study of landslide susceptibility mapping using landslide susceptibility index and artificial neural networks in the Krios River and Krathis River catchments (northern Peloponnesus, Greece). Bulletin of Engineering Geology and the Environment. 2015;74:27-45.
23. Ram P, Gupta V. Landslide hazard, vulnerability, and risk assessment (HVRA), Mussoorie township, lesser himalaya, India. Environment, Development and Sustainability. 2021;1-29.

24. Clerici A, Perego S, Tellini C, Vescovi P. A procedure for landslide susceptibility zonation by the conditional analysis method. Geomorphology. 2002;48(4):349-364.
25. Corominas J, Copons R, Vilaplana JM, Altimir J, Amigó J. Integrated landslide susceptibility analysis and hazard assessment in the principality of Andorra. Natural Hazards. 200;330:421-435.
26. Panchal S, Shrivastava AK. Landslide susceptibility mapping along highway corridors in GIS environment. In Smart Cities—Opportunities and Challenges: Select Proceedings of ICSC. Springer Singapore. 2019;79-89.
27. Panchal S, Srivastava AK. Expert based landslide susceptibility mapping for energy infrastructure planning. Journal of Information and Optimization Sciences. 2022;43(3):635-641.
28. Pourghasemi HR, Pradhan B, Gokceoglu C, Mohammadi M, Moradi HR. Application of weights-of-evidence and certainty factor models and their comparison in landslide susceptibility mapping at Haraz watershed, Iran. Arabian Journal of Geosciences. 2013;6:2351-2365.
29. Sifa SF, Mahmud T, Tarin MA, Haque DME. Event-based landslide susceptibility mapping using weights of evidence (WoE) and modified frequency ratio (MFR) model: A case study of Rangamati district in Bangladesh. *Geology,* Ecology, and Landscapes. 2020;4(3):222-235.
30. Van Westen CJ, Van Asch TW, Soeters R. Landslide hazard and risk zonation—why is it still so difficult?. Bulletin of Engineering geology and the Environment. 2006; 65:167-184.

Peer-review history:
The peer review history for this paper can be accessed here:
https://www.sdiarticle5.com/review-history/104210